SCIENTIFIC REPORTS

Cell sorting in a Petri dish controlled by computer vision

Z. Környei[1], S. Beke[2], T. Mihálffy[3], M. Jelitai[1], K. J. Kovács[1], Z. Szabó[4] & B. Szabó[4,5]

[1]Institute of Experimental Medicine of the Hungarian Academy of Sciences, Szigony u. 43, Budapest, H-1083 Hungary, [2]Laser Technology Laboratory, RIKEN - Advanced Science Institute, Wako, Saitama, 351-0198, Japan, [3]Furukawa Electric Institute of Technology, Vasgolyó u. 2-4, Budapest, H-1158 Hungary, [4]CellSorter Company for Innovations, Erdőalja út 174, Budapest, H-1037 Hungary, [5]Department of Biological Physics, Eötvös University, Pázmány Péter sétány 1A, Budapest, H-1117 Hungary.

Fluorescence-activated cell sorting (FACS) applying flow cytometry to separate cells on a molecular basis is a widespread method. We demonstrate that both fluorescent and unlabeled live cells in a Petri dish observed with a microscope can be automatically recognized by computer vision and picked up by a computer-controlled micropipette. This method can be routinely applied as a FACS down to the single cell level with a very high selectivity. Sorting resolution, i.e., the minimum distance between two cells from which one could be selectively removed was 50–70 micrometers. Survival rate with a low number of 3T3 mouse fibroblasts and NE-4C neuroectodermal mouse stem cells was 66±12% and 88±16%, respectively. Purity of sorted cultures and rate of survival using NE-4C/NE-GFP-4C co-cultures were 95±2% and 62±7%, respectively. Hydrodynamic simulations confirmed the experimental sorting efficiency and a cell damage risk similar to that of normal FACS.

Since the invention of the fluorescence-activated cell sorter (FACS)[1] in the 1960s the method gained widespread application both in research and medical diagnosis[2]. Several new developments appeared in the last decades including lab-on-a-chip versions of miniature FACS devices, called µFACS[3–6]. Cells move along with the fluid flow either in a microfabricated channel or in a nozzle with a diameter of 50–400 µm driven by a pressure of 10,000–400,000 Pa resulting in a flow velocity of 10 m/s[7]. The sort rate in a FACS can be 10,000 cells per second or more. In a µFACS it also exceeds 1,000 cells per second using piezoelectric actuation[6]. Although limited spatial resolution has been demonstrated in latest innovations[8] the fluorescent or scattered light of cells is normally detected without imaging the cells. There are several fluorescence-activated sorting mechanisms, among which the most successful is the electrostatic deflection of charged droplets containing single cells sprayed out from a nozzle. All these solutions are based on flow cytometry and turn to be difficult to apply if the number of cells is low not to mention single cell manipulations.

An inverted fluorescent microscope equipped with a digital camera is also capable of the automatic detection of live fluorescent cells[9] in a culture dish using appropriate image analyzing software. Such fluorescent cytometry is straightforward, and applied in specific fluorescent scanners or plate readers. The manipulation of cell cultures in a Petri dish or culture plate is, however, more demanding, especially on the single cell level. A recent innovation, called CellCelector™ can select and collect cells from culture dishes[10] using a micropipette. The micropipette is positioned by a robotic arm above the cell colony detected previously on the microscope stage, and picks up the colony or fraction of the colony. Subsequently the robotic arm moves the micropipette above an other culture dish transferring the cells into that. The application of the robotic arm results in a low sort rate. Although the ability of this technique for isolating cell colonies was demonstrated, single cell sorting with a reasonable speed and efficiency seems to be uneasy applying this method.

Semi-automated microinjection of adherent cells has been introduced[11] using the customary arrangement with a micropipette oriented diagonally relative to the optical axis and positioned by a motorized micromanipulator. Nevertheless such specialized complex devices are not very cost effective and it is hard to make extensive use of them. Image-controlled automated single cell manipulations, such as cloning, sorting or microinjection are still missing from the toolbox of most cell biologists.

We propose a simple accessory and method to overcome the technical difficulties of automated single cell manipulations on a microscope. If the goal is efficient single cell sorting by a micropipette, its positioning accuracy and delay are crucial parameters. In our case these are not limited by an extra robotic arm or micromanipulator. We argue that its simplicity, the precise 3D positioning of the micropipette and its relatively high sorting frequency make the device we used more suitable for automated single cell manipulations and sorting than
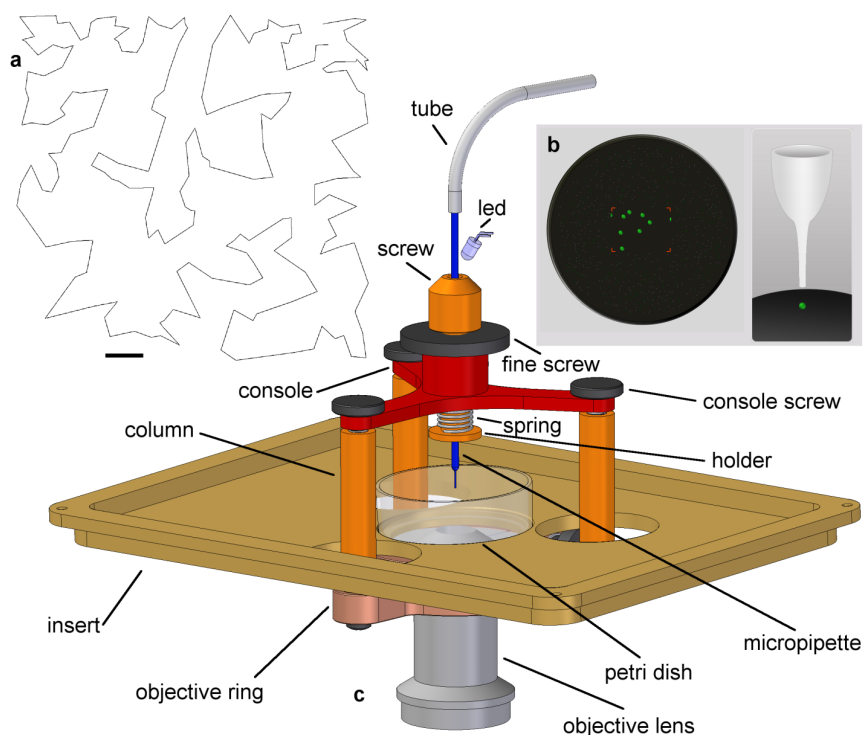
Figure 1 | Cell sorter micropipette. (a) Path of the micropipette during a typical sorting process, when 200 cells were picked up from the Petri dish. Scale bar: 100 um. (b) Hardware simulation module of the control software. Fluorescent cells are symbolized by green balls in the virtual Petri dish to be picked up by the micropipette. (c) Device for micropipette positioning. The glass micropipette is kept in the optical axis by a console mounted onto the objective lens with an objective ring, 3 columns and 3 console screws. Micropipette is fixed by a cylindrical holder inside the console tightened by a screw. The tip of the micropipette is illuminated by the light of the LED guided into the objective lens by the micropipette itself. Tip of the micropipette can be manually positioned into the focus of the objective lens using the fine screw counter the spring. The Petri dish sits in the insert. 3 columns span the insert at 3 circular holes on it enabling the horizontal displacement of the microscope stage and the Petri dish. The upper end of the micropipette is connected to a flexible tube leading to a syringe pump via the high speed 2-way normally closed liquid valve.

previous techniques like the CellCelector™. Although the very high sort rate achieved by flow cytometry cannot be obtained by our approach, sophisticated cell recognition is expected to induce extensive applications.

Results

Sorting procedure. We tested the prototype of a novel fluorescence-activated cell sorter device[12,13] applying a glass micropipette held by a console mounted onto the objective lens of a motorized inverted microscope (**Fig. 1**). This simple microscope accessory with appropriate software allows automated single cell manipulations controlled by computer vision. Vertical positioning accuracy of the micropipette is determined by the depth of field of the objective lens and the fine focus drive of the microscope. Using software calibration the horizontal positioning of the micropipette is as precise as the optical resolution of the microscope and the accuracy of the 2D motorized microscope stage.

We sorted live adherent mammalian cells cultured in 35 mm Petri dishes either on a thin layer of polydimethylsiloxane (PDMS) made hydrophilic by silanization or on bare glass. Phase contrast and fluorescent microscopic images of the culture were captured by a digital camera. A large area of the Petri dish was scanned by the 2D motorized stage. Software recognized cells in both phase contrast and fluorescent mosaic images merged from adjacent microscopic fields.

Selected fluorescent cells were visited one-by-one along a path computed by a traveling salesman algorithm (**Fig. 1a**) and picked up by the computer-controlled micropipette (**Fig. 1b,c**). To avoid crash the micropipette traveled between two cells at a height of ~100 µm above the surface. Cells were picked up by positioning

the next cell exactly under the aperture of the micropipette using the 2D motorized stage (**Fig. 2**). The upper end of the micropipette was connected to a plastic tube leading to a high-speed 2-way normally closed liquid valve. The other port of the valve was connected to a syringe controlled by a syringe pump. The micropipette and the tube were filled with deionized water prior to sorting. Before picking up the first cell culture medium was let into the micropipette to avoid the osmotic shock of cells. Using the focus drive the micropipette attached to the objective lens was lowered to get into the proximity of the surface before opening the fluid valve and picking up the cell in

Figure 2 | Cell sorter micropipette in action. Video shows the micropipette when picking up 40 cells from a 35 mm Petri dish held by the motorized microscope stage. Pick up process of single cells is accompanied by the tapping sound of the liquid valve as it opens for 8 ms.

approximately 1 µl culture medium. We applied the shortest available valve opening pulse of 8 ms to minimize the aspiration volume and the chance of removing neighboring cells. Soft PDMS coating assured the safe approach or touching the surface with the micropipette.

Sorting hardware. The objective lens of the microscopes was equipped with a micropipette holder device (CellSorter) keeping the capillary in the optical axis above the sample (**Fig. 1**). Capillary could be manually lifted or lowered relative to the objective lens using the fine thread. By this manual adjustment we positioned the tip of the capillary illuminated by the white LED to the focus plane of the objective lens with an accuracy limited by the depth of field of the objective lens. After this the capillary position was fixed relative to the objective lens and controlled by the microscope focus drive (MA- 42 with gearbox, Märzhäuser). Positioning accuracy of the micropipette parallel to the optical axis was determined by the depth of field (3.9 µm) of the objective lens and the fine focus mechanics with ~5 µm precision. Sorting resolution was optimal when the micropipette approached the surface to less than 10 µm. For fluid control we used a high speed 2-way normally closed liquid valve (AL3112, Asco) connected to a 50 ml syringe controlled by a syringe pump (NE-1000, New Era Pump Systems). This solenoid valve has a nominal response time of 5 ms. According to our test results the period of the shortest reproducible open state was 8 ms. We operated the valve with this parameter value in the sorting experiments. The vacuum in the syringe was adjusted by increasing the initial volume V_0 of air (corresponding to the ambient pressure p_0) to V inside at constant temperature resulting in a final pressure $p = p_0 V_0 / V$. $\Delta V = V - V_0$ was in the range of milliliters, orders of magnitude higher than the possible elastic deformation of the tubing and the volume of liquid drawn up from the Petri dish in a few pick up actions assuring constant vacuum in the syringe during the sorting experiments. When picking up more than 50 cells, we compensated the loss of vacuum in the syringe pump by increasing its volume with the estimated total volume (normally 50 µl) of the liquid drawn up from the Petri dish in 50 pick up actions. We limited the duration of the sorting process after the detection of cells to 15 minutes as motile cells can in turn leave their initial positions causing imperfect positioning of the micropipette. The temperature and pH of the culture medium also change without appropriate incubation leading to unfavorable conditions that can decrease the viability of cells in a longer period of time. We washed the whole fluid control system by sucking deionized water and 96% ethanol through the micropipette after each experiment to avoid contamination. Micropipettes could be reused in several experiments without clogging. Drying of the culture medium in the micropipette lifted out from the Petri dish could lead to clogging that could be usually resolved in water.

Cell detection and sorting software. Digital camera, motorized microscope stage, focus drive, syringe pump, liquid valve, and the pipette illumination were all controlled by a computer running the CellSorter software (CellSorter) with graphical user interface (GUI) on MS Windows OS. Using the scanning window of the GUI an area of the Petri dish defined by the operator is scanned by the motorized stage capturing adjacent phase contrast images to detect all cells in the area. The scan rate was 1 frame per second, i.e., a 10 × 10 mm² area of the Petri dish covered by 100 images could be scanned in 100 seconds. The scanning window offers a compensation algorithm in case the Petri dish is slightly tilted. After the operator gives the sharpest focus position of each 4 corner of the area to be scanned, the software fits a tilted plane resulting in sharp mosaic images in the end. System uses the same compensation method when the micropipette approaches a cell, i.e., the z position of each cell is corrected on the basis of the tilted plane of the Petri dish. User can switch on/off the transparent and fluorescent illumination in the

Microscope control window. As a next step the operator turns to the Analyzing window to detect cells either manually or automatically in the images. Parameters of automatic cell detection algorithm can be adjusted after clicking the Detection parameters button. To detect cells in phase contrast or fluorescent microscopic images the CellSorter software offers two automatic algorithms: the histogram median method applying standard image processing steps with median-based thresholding for object detection, and the local variance method[14]. Both methods have 3 input parameters: minimum and maximum cell size to be detected and threshold value for the histogram median method and sensitivity for the local variance method, respectively. High threshold or low sensitivity means less detected cells. Threshold and sensitivity values have to be optimized by the operator for the actual microscopic images to minimize the number of false negative and false positive detections. False detections can be corrected manually. The speed of detection is computer dependent. A Pentium dual-core 2.1 GHz processor with 4 GB RAM can analyze 4 microscopic images per second, which means that a 10 × 10 mm² area of the Petri dish covered by 100 images can be analyzed in about 25 seconds. Detection also can be performed manually by clicking cells with the PC mouse. Detected cells are indicated by green frames in the image. After detecting all cells in the phase contrast images the operator can scan the same area again in fluorescent mode to detect fluorescent cells. Position of cells previously scanned in phase contrast mode can be loaded and indicated in the fluorescent image. To avoid picking up unlabeled cells too close to a labeled one the user can choose to exclude cells that has a neighbor closer than the sorting resolution. After detecting fluorescent cells and excluding those that have a neighbor within a distance less than the sorting resolution the operator can proceed to the sorting window. Here a simulated annealing method calculates the shortest path to visit cells to be sorted by giving an approximate solution for the traveling salesman problem. The calculation took about 0.2 and 6.0 seconds in case of 100 and 1,000 cells, respectively. Adjustments with live cells preceding the first pick up action took ~5 minutes. CellSorter software running in hardware simulation mode can be downloaded from (http://facsinapetri.com).

Live cell sorting. We tested the sorting efficiency of the technique using three different mammalian cell types and two different fluorescent labels: normal 3T3 mouse fibroblasts mixed with their fellows stained by a lipophilic fluorescent dye, DiI; NE-4C neuroectodermal mouse stem cells mixed with NE-GFP-4C cells expressing green fluorescent protein (GFP) and primary culture of mouse astroglia cells with GFP-labeled microglia cells (**Fig. 3**). We needed to immobilize cells on the surface to apply the technique. We found that all three cell types could be readily sorted by the micropipette (**Fig. 3**) once the strength of cell adhesion had been optimized. Values of vacuum below were simply calculated as the experimentally controllable vacuum in the syringe minus the hydrostatic pressure of 2,000 Pa, when the syringe stayed 0.2 m lower than the cells. The actual vacuum in the fluid flow at the location of cells could be different from these values as a consequence of Bernoulli's law. (For further details see sections "Flow field measurement".) Weakly adherent NE-4C cells were easily picked up with a moderate vacuum of −6,000 Pa even after 1 d of seeding, when cells have reached full adherence. Although microglia cells adhered to the surface more strongly they could be picked up 1 d after seeding using a vacuum of −20,000 Pa, and viable cells could be regained as the MTT cell viability test showed. We quantified the rate of cell survival using 3T3 and NE-4C cells as it is described in the next section. Strongly adherent 3T3 cells were damaged if picked up with high vacuum 1 d after seeding. To gain viable 3T3 cells we sorted them 1 h after seeding using a vacuum of −12,000 Pa. During this time of incubation most 3T3 cells developed stable but not too strong attachment to the surface. Sucking force was adjusted
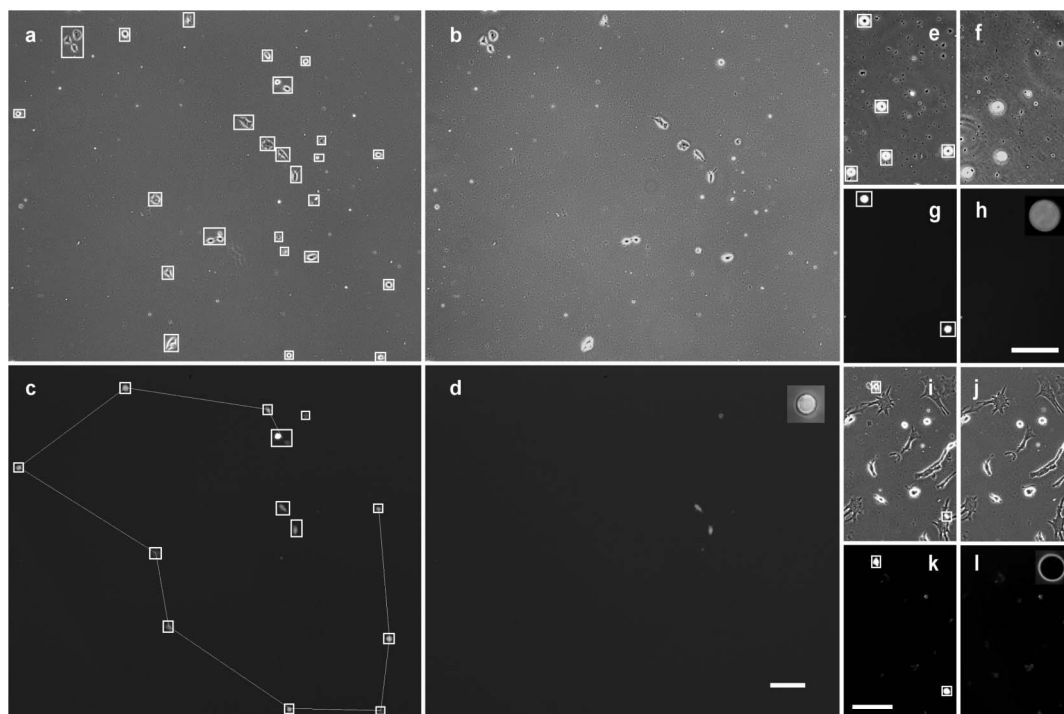
Figure 3 | Phase contrast and fluorescent images of cell cultures before and after sorting. (a,b,c,d) NE-4C, (e, f, g, h) 3T3, (i, j, k, l) astroglia-microglia cell cultures. (a, c, e, g, i, k) before, (b, d, f, h, j, l) after sorting, i.e., left panels show the cultures before and right panels after sorting. Aperture of the micropipette in action is shown in the insets of (d, h, l). A portion of NE-4C cells and all microglia cells were labeled by GFP. A portion of 3T3 cells were stained by DiI. Sorting process removed these fluorescent cells detected by software. Cells detected in phase contrast and in fluorescent images before sorting are indicated by white frames. Straight lines between cells in (c) show the path of the micropipette: three cells out of the path were excluded from sorting due to a neighbor closer than the sorting resolution of 50 μm, same as the inner diameter of the micropipette. We did not need to detect astroglia cells in phase contrast images (i) because GFP-labeled microglia cells could be removed even from the very close proximity of strongly adherent astroglia cells without perturbing them. Frames in (i) show microglia cells detected in panel k. Scale bars: 100 μm.

by the syringe pump and optimized to pick up minimum 90% of each cell type. Sorting resolution, i.e., the minimum distance between two cells from which one could be selectively removed was 50–70 micrometers, same as the micropipette aperture we used in the specific experiment. Labeled cells with a neighbor within the sorting resolution could be excluded from selection by software. The maximum number of cells picked up from a Petri dish in 15 minutes was about 1,000 eventually limited by the sorting speed of 1 cell per second. Sort rate was determined by software-to-hardware communication delays. An optimized hardware control for positioning is estimated to pick up more than 10 cells per second. To test some further cell types we also sorted HaCat human keratinocyte, HEK 293 human embryonic kidney cells, and mouse radial glia-like neural progenitors successfully (results not shown).

Cell survivability and sorting efficiency. After sorting, fluorescent cells were injected into and cultured further in a new culture dish. NE-4C and 3T3 cells were apparently viable and proliferated in the new culture dish leading to monocultures of fluorescent cells without unlabeled cells. As the viability of microglia cells is not straightforward on the basis of cell morphology, we completed the MTT test. Most microglia cells were viable according to their reductive capacity after sorting.

To quantify the sorting efficiency of the technique and the rate of cell survival we used unlabeled 3T3 and NE-4C cells. In a preliminary experiment we picked up several hundreds of 3T3 cells with a micropipette having 62 μm aperture and a vacuum of −12,000 Pa after the automatic detection of cells. **See supplementary material.** We found a pick up efficiency of 98% (number of cells selected: 291) and a rate of survival of 65% (number of cells picked up: 284).

However, the rate of cell survival emerged to be unstable in further experiments in case of both cell types. Cell adherence stronger than the forces maintaining cell integrity can result in cell damage, when the pipette picks up the cell. In this case minor parts of the cell remain on the surface. Long cell processes reaching out of the micropipette aperture can be broken (**Fig. 4**). We applied a brief trypsin-EDTA treatment of fully adhered cells before sorting in order to achieve a stable rate of survival in cultures 1 d after seeding (**Table 1**, **Fig. 5**). We measured a rate of survival of $88\pm16\%$ and $66\pm12\%$ for NE-4C and 3T3, respectively, with a micropipette aperture of 69 μm. We also investigated the effect of the strength of vacuum on cell survival. In the range of $[-4,700; -12,900]$ Pa we found that the increasing vacuum did not alter the rate of cell survival.

Sorting a larger number of cells from NE-4C/NE-GFP-4C co-cultures we measured the indicators of sorting efficiency including sorting purity, cell viability and the purity of sorted cultures (**Table 2**). Sorting purity and pick up efficiency was $95\pm2\%$ and $93\pm5\%$, respectively. Average rate of survival was $62\pm7\%$. Average purity of the sorted culture (number of fluorescent cells divided by the total number of cells) was $95\pm2\%$.

We also performed experiments to investigate the rate of survival of primary glial cultures prepared from CD1 mouse. 3 min pretreatment of cells with trypsin-EDTA resulted in 100% rate of survival in an experiment with cells selected for sorting and picked up.

To compare the viability of sorted cells to cells not sorted but passed over a new Petri dish from the PDMS surface applying the usual routine method with trypsin-EDTA we measured the rate of survival after normal passage as detailed in section "Cell viability assays". The control experiment resulted in a rate of survival of
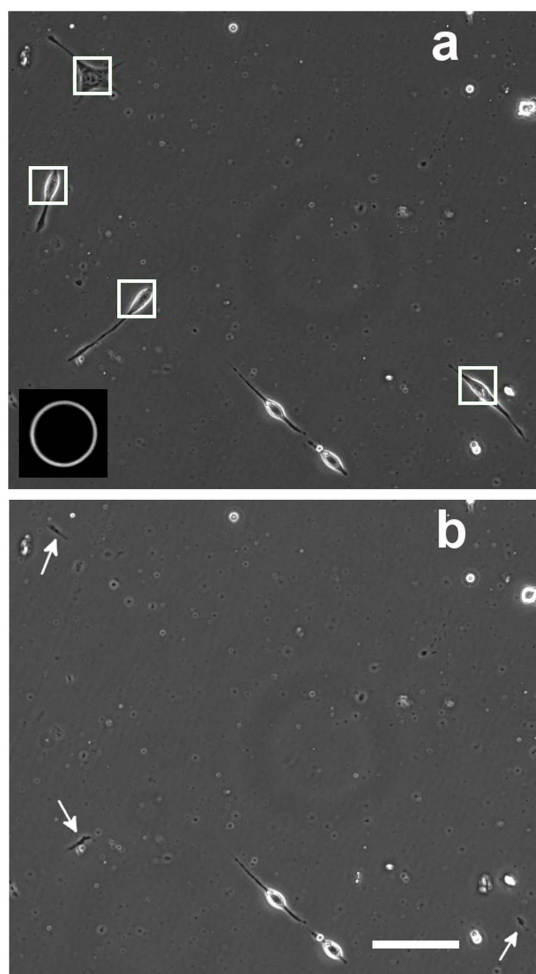
Figure 4 | Cell damage. 3T3 cell culture before (a) and after (b) picking up 4 cells indicated by white frames in (a). Note the cell processes remaining on the surface highlighted by the arrows in (b). Only one cell out of four survived this sorting. Aperture of the micropipette in action is shown in the inset of (a). Scale bar: 100 μm.

70±4% and 76±5% for NE-4C and 3T3 cells, respectively. These values are comparable to the survival rates of sorting.

Flow field measurement. To gain a deeper understanding of the pick up process we characterized experimentally the flow field of the micropipette above the PDMS surface using particle image velocimetry[15]. Flow tracking particles in microfluidics[16] have to be small enough to follow the flow without disturbing the flow field and also have to be large enough to avoid Brownian motion and imaging difficulties. We applied 2 μm fluorescent beads suspended in water. Beads with this size could be easily detected with our optical setup, and were small as compared to the pipette aperture and the cell size. The tip of the micropipette was positioned to a height of approximately 10 μm above either the PDMS or the bare glass surface in the Petri dish. We opened the liquid valve for 1 s to let the flow enter into the micropipette. A vacuum of −8,700±12 Pa induced by the syringe pump generated a flow rate of 6.4±0.1 μl/s, which means an average flow velocity of 1.7±0.03 m/s at the tip of the micropipette with an inner diameter of 69 μm. The drop of pressure in the plastic tubing according to the Hagen-Poiseuille law was only 73 Pa. As a first approximation to calculate the pressure at the tip of the micropipette one can use Bernoulli's equation and gain a value of −10,100 Pa. This approximation leaves out of consideration the friction and the inhomogeneity of

the flow field in the micropipette. The flow velocity at the tip of the micropipette infers a Reynolds number of 132 indicating laminar flow as the transition Reynolds number in a boundary layer flow over a flat plate is 500,000, and in a pipe the flow is also laminar if the Reynolds number is under 2,300. To record the finite displacement of beads we focused the microscope 10 μm above the plane of the PDMS surface and captured images with an exposition time of 10 ms. Beads moving with the flow were observed in microscopic images (**Fig. 6a**), and the velocity of flow was determined on the basis of bead displacements as a function of radial distance from the axis of the micropipette. Some beads adhered strongly to the surface remained stationary in the flow. Beads tended to adhere to the surface of the Petri dish out of the micropipette close to its edge. This observation cannot be explained by the flow field simulations. The effect might be explained by beads arriving to the micropipette edge with a streamline nearly perpendicular to the surface of the Petri dish and here crossing the highly curved streamlines due to the inertial force and then hitting the surface.

Numerical simulations of the flow field. We constructed a model (**Fig. 6b**) to simulate the flow close to the tip of the micropipette. Input parameters were the geometry and vacuum values applied in the live cell sorting and bead displacement experiments. The result of numerical simulations were consistent with both the experimentally measured flow rate and the velocity of the flow field (**Fig. 6c**). To estimate the force acting on a single cell under the micropipette and cells farther from that we calculated the pressure (**Fig. 6d, f**) at the bottom of the Petri dish as a function of radial distance from the axis of the micropipette. We found a very sharp drop of pressure at the edge of the micropipette and a plateau in the mid region explaining both the high pick up efficiency in case of cells positioned precisely under the micropipette and the sorting resolution comparable to the diameter of the micropipette. The estimated lifting force acting on a typical cell with a diameter of 20 μm under the micropipette was calculated as the product of the vacuum of [−4,000;−12,000] Pa at the location of cells corresponding to the experimentally controlled values of [−4,700; −12,900] Pa and the cell surface. The resultant 1.3 − 3.8 μN is an order of magnitude higher than the typical adhesion force of single cells[17] ensuring a high ratio of cells picked up. We calculated also the shear stress (**Fig. 6e, g**), which shows high values on the surface under the edge of the micropipette. Sharp drop of the shear stress similarly to the pressure reinforces that cells out of the range of the micropipette are almost unaffected by the flow. Energy dissipation rate (EDR) an indicator of the damaging impact of the flow[18] on cells was calculated from simulations. The experimentally measured vacuum dependence of cell survival rate (**Fig. 7a, b**) was correlated to the EDR values. We also explored the regions of the flow field that can possibly damage cells. A cell in the middle zone of the micropipette is exposed to EDR values (**Fig. 7c, d**) comparable to those of normal FACS falling into the range of 10^7 W/m^3 [18]. Although a higher vacuum increases the EDR, this effect is less critical than the spatial variance of EDR as shown in **Fig. 7c**. Simulations show that cells either adhered to the surface under the edge of the micropipette or getting very close to the edge of the micropipette may be damaged by the high EDR (**Fig. 7e**).

Numerical simulations have been performed with the Finite Element software package COMSOL using the stationary laminar incompressible Navier-Stokes solver with the viscosity of water (8.9 10^{-4} Pas) based on the geometry and vacuum value applied in the live cell sorting and bead displacement experiments. The calculation domain was assumed to have cylindrical symmetry with an axial dimension of 200 μm and a radial dimension of 600 μm. The micropipette with an inner radius of 31.5 or 34.5 μm was positioned coaxially with the symmetry axis. The wall thickness of the micropipette positioned 5–10–20 μm above the surface was 5 μm. The edge of the

Table I | Sorting efficiency and rate of cell survival of unlabeled cells. After a brief (30–60 s) trypsin-EDTA treatment we marked 3–5 cells manually in an image of the culture captured in the phase-contrast mode of the microscope. We adjusted the vacuum in the syringe connected to the micropipette with an aperture of 69 μm, and picked up cells automatically. 0 vacuum means ambient pressure in the syringe. Cells were then injected to a cloning cylinder placed into the middle of a new Petri dish to make easier the subsequent search for cells. 2 h later we counted live cells in the new Petri dish. Pick up efficiency was calculated as the ratio of the number of selected cells picked up and the number of all selected cells. Average pick up efficiency was 93±4% and 100% for 3T3 and NE-4C, respectively. In some experiments the micropipette picked up extra cells from the neighborhood of cells selected for sorting. The number of these cells is indicated after the + signal in the 'Number of cells picked up' column. Pick up rate of cells not selected for sorting is the ratio of this number and the number of all selected cells. Average pick up rate of unselected cells was 11±12 % and 6±6% for 3T3 and NE-4C, respectively. The rate of survival was calculated as the ratio of the number of cells survived and the number of cells picked up including also unselected cells. Average rate of survival was 66±12 % and 88 ±16% for 3T3 and NE-4C, respectively. Average rates were calculated as the sample mean weighted by the denominator of each ratio, i.e., the number of input cells. The error of the mean was approximated by the weighted sample variance divided by the square root of the number of experiments

Cell type	Duration of trypsin-EDTA treatment (s)	Vacuum (10^5 Pa)	Number of cells selected for sorting	Number of cells picked up	Pick up efficiency	Pick up rate of cells not selected for sorting	Number of cells survived	Rate of survival
3T3	30	0.09	4	4	1	0	1	0.25
3T3	30	0.069	5	4	0.8	0	3	0.75
3T3	30	0.110	3	3	1	0	3	1.00
3T3	30	0.129	4	4	1	0	1	0.25
3T3	40	0.090	3	2	0.67	0	2	1.00
3T3	40	0.110	3	3+3	1	1	6	1.00
3T3	30	0.090	3	3	1	0	2	0.67
3T3	30	0.110	3	3	1	0	1	0.33
NE-4C	60	0.047	4	4	1	0	4	1.00
NE-4C	60	0.090	4	4	1	0	3	0.75
NE-4C	60	0.047	4	4	1	0	3	0.75
NE-4C	60	0.090	4	4+1	1	0.25	5	1.00

micropipette was simulated by a rounded shape with a circular cross-section. We used a triangular mesh generated with a maximum element size of 10 μm in the entire domain and a maximum size of 0.3 μm at the bottom boundary and 0.2 μm at the edge of the micropipette. The top boundary of the pipette was an outlet with a fixed input pressure from the experiments. The cylinder surface (r=600 μm) was an inlet boundary and the pressure was fixed to 0. We set slip wall boundary condition on the top boundary outside
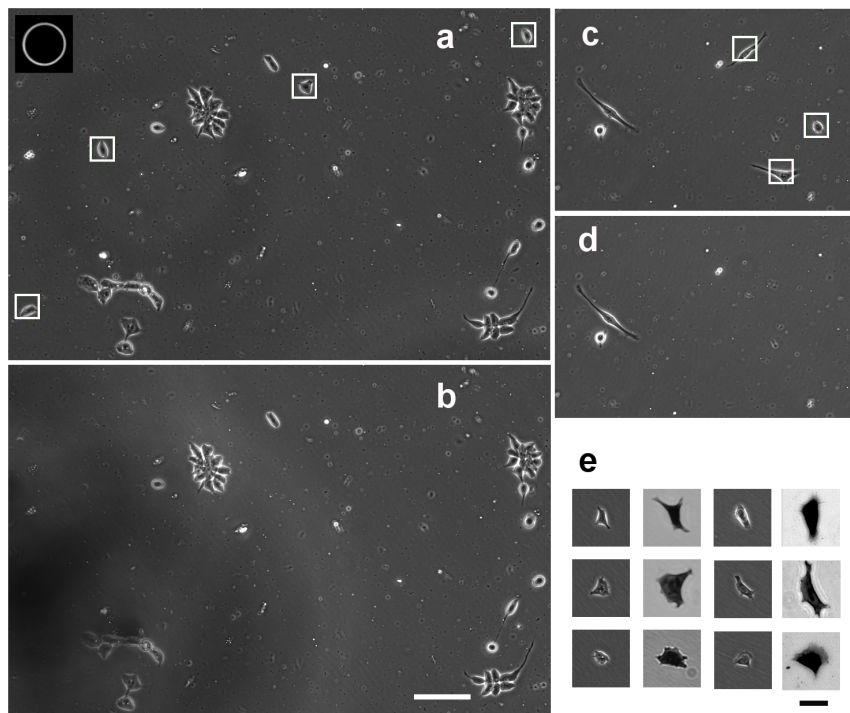

Figure 5 | Cell survival. NE-4C (a, b) and 3T3 (c, d) cell cultures before (a, c) and after (b, d) sorting, i.e., top panels show the cultures before and bottom panels after sorting. Cells selected manually for sorting are indicated by white frames. (e) shows cells surviving 2 h after sorting. First column from the left: phase-contrast image of the 3 out of 4 NE-4C survivors. Second column: same cells stained with methylene blue and captured with 20× objective lens. Third and fourth column show the 3 out of 3 3T3 survivors. Cultures were pretreated with trypsin-EDTA before sorting. Aperture of the micropipette in action is shown in the inset of (a). Scale bar for all phase-contrast images in (b): 100 μm. Scale bar for bright field images in (e): 25 μm.

Table 2 | Sorting efficiency with larger number of cells. We used a mixed culture of unlabeled NE-4C and fluorescent NE-GFP-4C cells in 6 experiments with a total number of 311 cells selected for sorting. After a brief (30s) trypsin-EDTA treatment software detected the cells in a merged image of the culture captured in both phase-contrast and fluorescent modes of the microscope. Vacuum was in the range of [−9,000; −11,000] Pa in the syringe connected to the micropipette with an aperture of 70 μm. After the software excluded those cells that were closer to other cells than 70 μm we picked up fluorescent cells automatically. Cells were then injected to a 6 mm PDMS cylinder attached onto a glass cover slip to make easier the subsequent search for cells. 2 h later we counted live fluorescent and unlabeled cells on the cover slip. Pick up efficiency was calculated as the ratio of the number of selected cells picked up and the total number of selected cells. Sorting purity is the ratio of the number of fluorescent cells and the total number of cells picked up. Average sorting purity and pick up efficiency was 95±2% and 93±5%, respectively. In some experiments the micropipette picked up extra fluorescent cells from the neighborhood of cells selected for sorting. The number of these cells is indicated after the + signal in the 'Number of fluorescent cells picked up' column. The rate of survival was calculated as the ratio of the number of cells survived and the number of cells picked up including also unselected cells. Average rate of survival was 62±7%. Average purity of the sorted culture (number of fluorescent cells divided by the total number of cells) was 95±2%. Average rates were calculated as the sample mean weighted by the denominator of each ratio, i.e., the number of input cells. The error of the mean was approximated by the weighted sample variance divided by the square root of the number of experiments

Number of cells selected for sorting	Number of fluorescent cells picked up	Number of unlabeled cells picked up	Sorting purity	Pick up efficiency	Number of fluorescent cells survived	Number of unlabeled cells survived	Rate of survival	Purity of the sorted culture
86	85+2	1	0.99	0.99	40	0	0.45	1
53	38	2	0.95	0.72	16	1	0.42	0.94
65	59	10	0.86	0.91	49	7	0.83	0.88
19	19	1	0.95	1	14	1	0.74	0.93
42	42	0	1	1	25	0	0.6	1
46	46+1	1	0.98	1	37	1	0.79	0.97

the pipe, while we prescribed no-slip condition on the bottom boundary and on the wall of the micropipette. **See supplementary material.**

Discussion

We found that automated sorting of single cells in a Petri dish can be easily realized on a motorized microscope with a simple accessory for micropipette positioning and fluid control after the recognition of cells by computer vision. Sorting resolution, i.e., the minimum distance between two cells from which one could be selectively removed was 50–70 micrometers, same as the micropipette aperture we used in the specific experiment. The maximum number of cells picked up from a Petri dish was about 1,000 limited by our current sorting speed of 1 cell per second.

Cell adhesion strength is a crucial parameter of the technique: cells adhered to the surface too weakly or strongly cannot be efficiently sorted. We used three cell types with different adhesion strengths to demonstrate that under adequate conditions both weakly and strongly adherent cells can be readily sorted by the method. Before sorting cell adhesion has to be optimized for the different cell types.

Without the pretreatment of cells before sorting the rate of cell survival emerged to be unstable that we attribute to the loss of cell integrity in a variable number of cells. A brief trypsin-EDTA treatment of fully adhered cells before sorting stabilized the rate of survival. To quantify the rate of cell survival we used low number of 3T3 mouse fibroblasts and NE-4C neuroectodermal mouse stem cells, and measured 66±12% and 88±16%, respectively. Sorting a larger number of cells from NE-4C/NE-GFP-4C co-cultures we measured a sorting purity and pick up efficiency of 95±2% and 93±5%, respectively. Rate of survival was 62±7% with a purity of 95±2%. These values are comparable to the survival rate of cells after normal passage with trypsin-EDTA without sorting: 76±5% and 70±4% for 3T3 and NE-4C, respectively. As a more relevant comparison, the rate of cell survival in normal FACS is in the range of 70–80%[19]. A higher vacuum did not alter the rate of survival indicating that the shear force or EDR inside the pipette is not critical. We argue that cells can be rather damaged during the detachment from the surface, when a part of the cell remains attached to the surface. This happens if the cell adhesion is stronger than the forces maintaining the integrity of the cell. Trypsin-EDTA treatment could overcome this

problem. Simulations confirmed that the increasing vacuum value is less critical than the right positioning of the micropipette. Cells positioned under the edge of the micropipette may be damaged by the high EDR at this region.

The positioning accuracy of the device can be improved to achieve the submicron regime by an objective lens with high numerical aperture and piezoelectric actuation of the microscope stage and the objective lens. Sort rate was determined by software-to-hardware communication delays. An optimized hardware control for positioning is estimated to pick up more than 10 cells per second. Further improvement may be achieved with the application of specialized motorized stage and objective actuation with lower travel ranges and mass. Our current precision mechanics has a maximal travel speed in the 1–10 mm/s range that also becomes a bottleneck in case of a throughput of 10 cells per second. The opening time of the valve can be decreased to ~1 ms using an extra high speed fluid valve, which sets a maximum sort rate in the kHz range.

The method is capable of isolating a subpopulation of cells expressing fluorescent or luminescent markers or cells labeled by fluorescent molecular probes highlighting specific cellular activities. The device will be able to collect single cells for further cultivation, cloning, RNA or protein preparation, and to sort also fixed cells after immunocytochemical preparation. Detection of cells with a characteristic feature in their microscopic image using computer vision similarly to face recognition in digital photos and subsequent automated manipulation, e.g., sorting or microinjection will be feasible. If combined with time-lapse imaging or even with simultaneous RNA screening[20], the device can isolate cells with specific phenotypes.

Methods

Micropipette pulling. We used a Model P-87, Flaming/Brown micropipette puller (Sutter) to gain micropipettes with an inner diameter of 50–70 micrometers at the tip from the PG150T-10 glass capillaries with an outer diameter of 1.5 mm (Clark Electromedical Instruments). We used the following parameters: Heat= ramp value, Pull=0, Velocity=15, Time=180, and measured the micropipette aperture on a microscope with our sorting hardware described in section "Sorting hardware". Micropipette aperture could be increased by lowering the velocity parameter of pulling.

PDMS surface for cell cultures. 35 mm plastic Petri dishes (Greiner) were covered with PDMS: poly(dimethylsiloxane)[21] as follows. A drop of 0.1 g PDMS liquid premixed in a 10 : 1 ratio by weight of silicone base and curing agent (Sylgard 184,
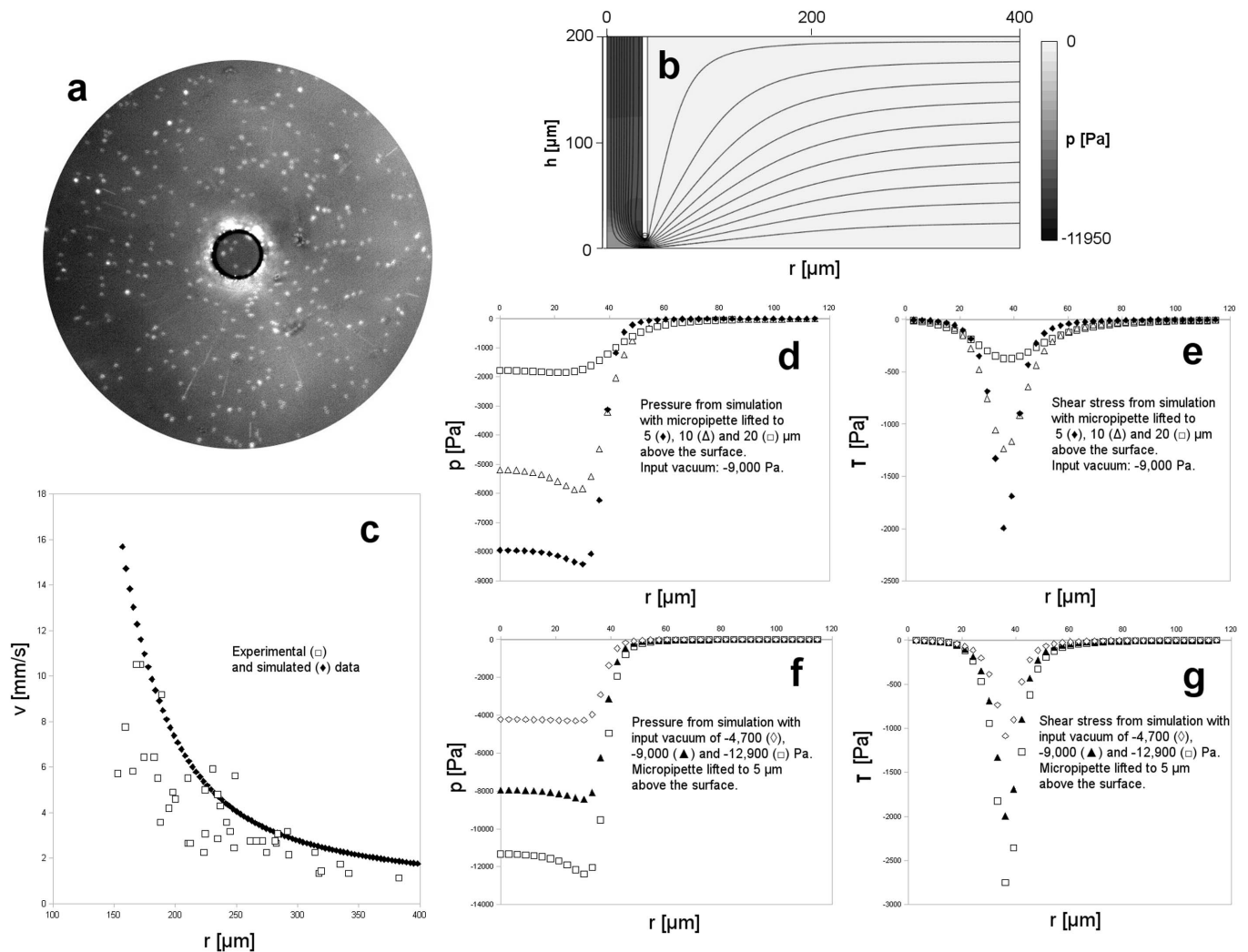
Figure 6 | Flow field of the micropipette. (a) Fluorescent beads at the bottom of the Petri dish moving with the flow generated by the micropipette with an aperture of 69 μm shown in the center. Moving beads 10 μm above the surface appear as narrow radial lines, beads adhered to the surface appear as out-of focus dots as the objective was focused 10 μm above the surface. Beads tend to adhere to the surface out of the micropipette close to its edge. Vacuum: −8,700 Pa, exposition time: 10 ms, bead size: 2 μm. (b) Side view of the simulated velocity and pressure of flow generated by a vertical micropipette in the proximity of a horizontal plane with the same geometry as applied in the experiment and input vacuum of −9,000 Pa. Panel size: 0.4 × 0.2 mm. Velocity and pressure is indicated by streamlines and color code, respectively. The darker color means the lower pressure from 0 to −11,950 Pa. (c) Radial flow velocity as a function of radial distance measured from the center of the micropipette. Experimental (□) and simulated (◆) data calculated from the displacement of beads shown in (a) and from the model outlined in (b) at a height of 10 μm above the surface, respectively. (d) Pressure on the surface as a function of radial distance calculated from the simulation with 3 different values: 5 (◆), 10 (Δ) and 20 (□) μm of distance between the surface and the micropipette. Vacuum: −9,000 Pa. (e) Similar plot to (d) for the shear stress on the surface. (f) Pressure on the surface as a function of radial distance calculated from the simulation with 3 different values: −4,700 (◇),−9,000 (▲) and −12,900 (□) Pa of vacuum. Distance between the micropipette and the surface: 5 μm. (g) Similar plot to (f) for the shear stress on the surface.

Dow Corning) was placed on the center of the dish. Then the Petri dish was attached onto the center of a custom modified desktop laboratory centrifuge (Medifuge, Heraeus), and spin coated at 1000 RPM for 2 minutes. As a result we gained a PDMS film with a thickness of 0.1 mm covering the bottom of the Petri dish. We kept the PDMS covered dishes at room temperature for 72 h. Hardened PDMS surfaces were washed with 96% ethanol (Molar), and treated with 0.1% DETA (trimethoxysilylpropyldiethylenetriamine, Fluorochem)[22] for 30 minutes to make them hydrophilic. We removed the DETA, and washed the surface with 0.1 M phosphate buffered saline (PBS).

Cell cultures for sorting. *NE-4C neuroectodermal stem cells.* The neuroepithelial cell lines, NE-4C (ATCC; CRL-2925) and NE-GFP-4C (ATCC; CRL-2926) had been established from the cerebral vesicles of 9-day-old mouse embryos lacking the functional p53 genes. The cells display neural stem cells properties as they differentiate to neurons and astrocytes when exposed to all-trans retinoic acid. NE-4C cells were maintained in MEM supplemented with 10% FCS, 4 mM glutamine and 40 mg/ml gentamycin (Sigma), at 37°C temperature with 5% CO2. Subconfluent cultures were regularly passaged by trypsinization (0.05% trypsin in PBS) into poly-L-lysine coated Petri dishes.

Primary astroglia-microglia cultures. Mixed astroglia-microglia cell cultures were obtained from the forebrains of neonatal (P1-3) CD1 or transgenic mice expressing eGFP in knock-in constructs within the CX3CR1 gene[23]. Meninges were removed and the tissue was minced with razor blades. The tissue pieces were subjected to enzymatic dissociation, using 0.05% w/v trypsin and 0.05% w/v DNase I for 10 minutes at room temperature. The cells were plated onto poly-L-lysine coated plastic surfaces and were grown in MEM supplemented with 10% FCS, 4 mM glutamine and 40 μg/ml gentamycin (Sigma) in humidified air atmosphere containing 5% CO_2, at 37°C. The culture medium was changed on the first two days and every second-third day afterwards. The cells were subjected to cell sorting after minimum 3 weeks in culture, when the number of microglial cells was approx. 25% of the total cell number.

3T3 cells. Mouse embryonic fibroblasts (ATCC; CCL-92) were grown in MEM supplemented with 10% FCS (Sigma), according to the guidelines of the ATCC Cell Biology Collection. A subpopulation of the cells was stained by the lipophilic fluorescent dye, DiI (10 uM, 30 minutes at 37°C, Invitrogen).

Cell cultures on PDMS or bare glass surfaces. 10^4–10^5 GFP labeled or DiI stained and normal cells were seeded on the DETA coated PDMS surface in minimum essential
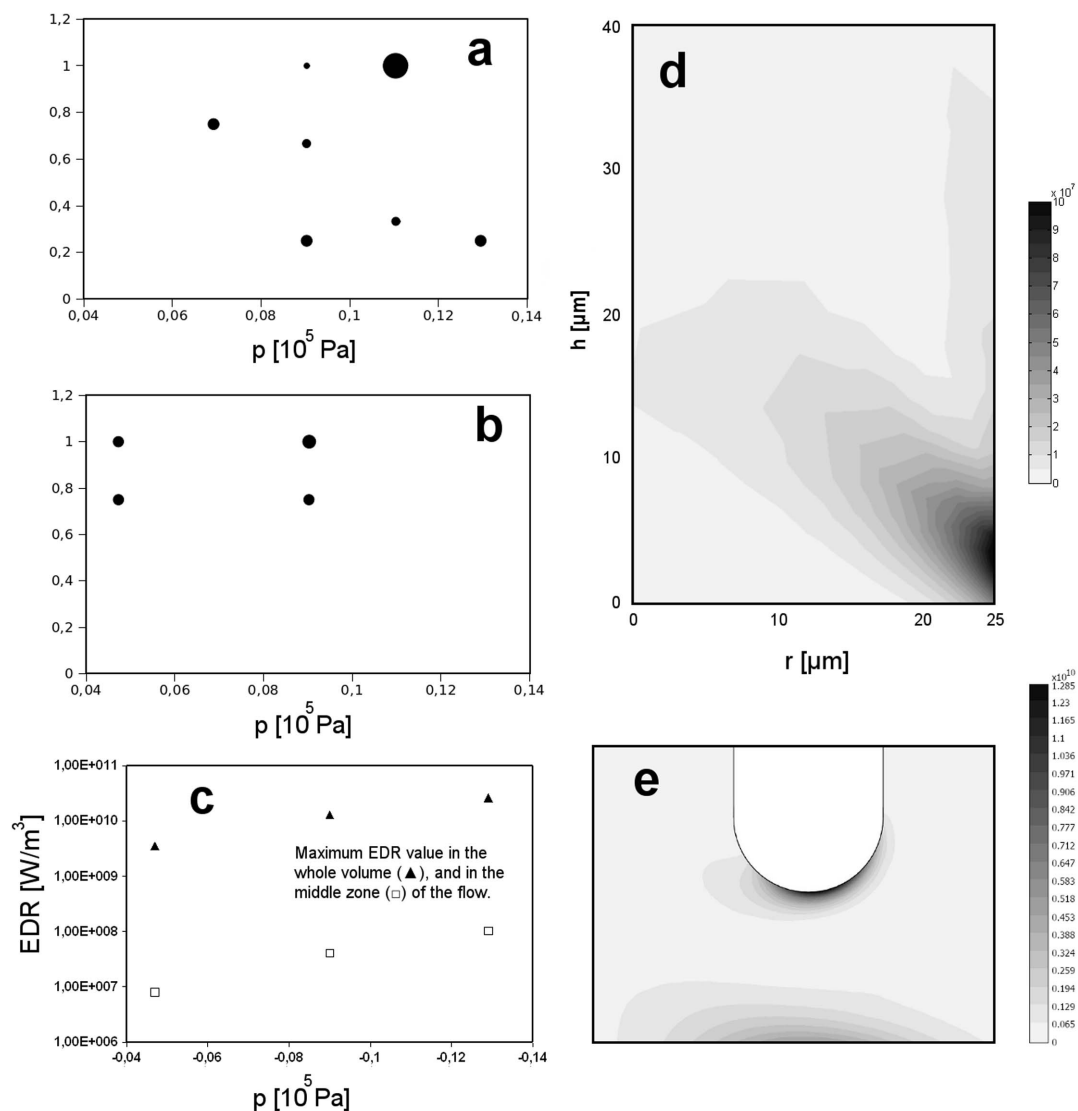
Figure 7 | Hydrodynamic impact on cell survival. Rate of 3T3 (a) and NE-4C (b) cell survival is presented as a function of vacuum generated by the syringe during sorting. Bubbles in the graph correspond to data in **Table 1**. Bubble diameter is proportional to the sample size, i.e., the number of cells picked up. (c) Maximum energy dissipation rate (EDR) calculated from simulation as a function of vacuum presented in logarithmic scale. Maximum EDR value was determined in the whole volume (▲) and also in the middle zone of the flow (□) shown in (d) up to r=20 μm. The vacuum dependence of EDR is weaker than its spatial variation. (d) EDR map of the flow field in the middle zone of the micropipette up to r=25 μm with a vacuum of −9,000 Pa. (e) EDR map of the flow field close to the edge of the micropipette shown in white in the middle of the image. In (c, d, e) the micropipette aperture and wall thickness are 69 μm and 5 μm, respectively. Distance between the micropipette and the surface is 5 μm. EDR value is indicated in color code in W/m³ units in (d) and (e) from 0 to 10^8 and from 0 to $1.285*10^{10}$, respectively.

medium (MEM) supplemented with 10% FCS (Sigma). This number of cells resulted in a culture containing a reasonable ratio of cells separated from others by more than 50–60 micrometers. To let NE-4C and primary astroglia-microglia cells fully adhere to the surface we kept the cultures at 37°C in 5% CO_2 atmosphere with 100% relative humidity in a laboratory incubator (HeraCell, Heraeus) for 24 h. To reach a culture of 3T3 cells moderately attached to the surface, cells were kept in the incubator for either 1 h or 1 d after seeding. In case of 1 d incubation of 3T3 cells we applied trypsin-EDTA pretreatment as follows. Before sorting culture medium was exchanged to remove cells floating in the Petri dish. When measuring the sorting efficiency of the mixed culture of NE-4C and NE-GFP-4C cells we seeded cells into bare 35 mm glass bottom Petri dishes (Ibidi) 4–5 hours before sorting.

Trypsin-EDTA pretreatment before sorting. To achieve a stable rate of 3T3 and NE-4C survival of fully adhered cells 1 d after seeding we treated the cultures with 1× trypsin-EDTA solution (Gibco, 25300) at room temperature. 2 ml culture medium was removed, cultures were washed with 1 ml PBS, and 1 ml trypsin-EDTA was injected. We removed trypsin-EDTA after 30–60 s, gently washed the cultures with 1 ml culture medium, and changed it to 2 ml fresh medium. Sorting was done 5–20 minutes after the trypsin-EDTA treatment.

Culture of selected cells. We injected the culture medium with the selected cells from the micropipette into a 96-well culture plate or 35 mm Petri dish (Greiner). When sorting only a few cells we used either a polystyrene cloning cylinder (Sigma, Scienceware) with an inner diameter of 6.4 mm containing 0.1 ml culture medium or a custom made PDMS cylinder attached onto a glass cover slip. We placed the cloning cylinder into the middle of the Petri dish to make the subsequent search for cells easier. After 2 h the medium was changed to remove any possible cell debris. Culture was either fixed for cell counting or kept at 37°C in 5% CO_2 atmosphere with 100% relative humidity in the laboratory incubator for 3–7 days to observe cell survival and proliferation rate after sorting.

Cell viability assays. The viability of individual primary microglial cells subjected to cell sorting was determined by MTT-test[24]. Briefly, sorted cells were treated with 3-(4,5-dimethylthiazol-2-yl)-2,5-diphenyltetrazolium bromide (MTT) in a final concentration of 250 ug/ml. After 4 or 24 h incubation formazan crystal formation was observed in living cells with considerable reductive capacity.

Preliminary measurement of 3T3 cell survival rate with hundreds of cells was carried out 1 h after seeding without trypsin-EDTA pretreatment. We counted cells survived 1 d after sorting by fixing the culture with 4% paraformaldehyde (PFA) for 20 min, and visually detecting cells using the phase contrast mode of the microscope.

To quantify the ability of the technique to sort low number of cells we measured the rate of survival of 3 to 5 NE-4C and 3T3 cells. In these experiments cultures were briefly pretreated with trypsin-EDTA before sorting. We counted survivals 2 h after sorting. Cultures were fixed with 4% PFA for 20 min at room temperature. As the normal cell adhesion to the surface of the culture dish is a result of a complex biological process that happens only in live cells, we considered adhered cells with normal morphology alive. Image of each adhered fixed cell was captured in the phase-contrast mode of the microscope after their visual detection. Cell doublets very close to each other were identified as sisters from a cell dividing after sorting, and counted as single survivor. We also stained the cultures with the application of 0.5% methylene blue (Reanal) for 30 min at room temperature for the bright field imaging of fixed cells.

We measured the rate of survival in 2–2 parallel control cultures of NE-4C and 3T3 cells without sorting. We seeded approximately 10,000 cells on the DETA coated PDMS surface in minimum essential medium (MEM) supplemented with 10% FCS (Sigma) in 35 mm plastic Petri dishes (Greiner). After 1 d the cultures were washed with PBS, flushed with fresh culture medium and an area of 38 mm^2 in the middle of the dish was scanned in phase-contrast mode. We counted cells in the mosaic image of this area by visual detection. Cultures were then washed with PBS, treated with 1 ml preheated 1× trypsin-EDTA at room temperature for 2.5 and 2 min in case of NE-4C and 3T3, respectively. Then we removed the trypsin-EDTA and suspended all the cells in 1 ml culture medium using a 1 ml pipette. 0.5 ml cell suspension was passed over a new plastic Petri dish (Greiner) without PDMS coating. Cultures were kept at 37°C in 5% CO_2 atmosphere with 100% relative humidity in the laboratory incubator for 2 h. We washed the cultures with PBS and added fresh culture medium before scanning again the mid region of the new Petri dishes with an area of 38 mm^2. Cells were counted again by visual detection in the mosaic images captured in phase-contrast mode.

Imaging. For the phase contrast and fluorescent imaging of cell cultures we used Leica DM IRB and Zeiss Axio Observer A1 inverted microscopes with N Plan 10×/0.25 Ph1 and EC Plan-Neofluar 10×/0.3 Ph1 objective lens, respectively. Microscopes were equipped with Scan IM 120x100 motorized stage and focus drive (Märzhäuser) controlled by Tango control unit (Märzhäuser) with a maximal speed of 9.2 and 1.9 mm/s for each. For image acquisition we used an Olympus DP70 and a Qcam Retiga 1300 cooled CCD camera.

Flow field measurement. We measured the displacement of microbeads in the flow field of the micropipette. We injected 2 µl suspension of fluorescent red polystyrene beads with a diameter of 2 µm (L3030, Sigma) into 2 ml deionized water on the DETA coated PDMS surface to visualize the horizontal flow at the bottom of the 35 mm Petri dish.

1. Herzenberg, L. A., Sweet, R. G. & Herzenberg, L. A. Fluorescence-activated cell sorting. *Sci. Am.* **234**, 108–117 (1976).
2. Herzenberg, L. *et al.* The history and future of the fluorescence activated cell sorter and flow cytometry: a view from Stanford. *Clin. Chem.* **48**, 1819–1827 (2002).
3. Fu, A. Y., Spence, C., Scherer, A., Arnold, F. H. & Quake, S. R. A microfabricated fluorescence-activated cell sorter. *Nat. Biotechnol.* **17**, 1061–1062 (1999).
4. Wolff, A. *et al.* Integrating advanced functionality in a microfabricated high-throughput fluorescent-activated cell sorter. *Lab Chip.* **3**, 22–27 (2003).
5. Ateya, D. A. *et al.* The good, the bad, and the tiny: a review of microflow cytometry. *Anal Bioanal Chem.* **391**, 1485–1498 (2008).
6. Cho, S. H., Chen, C. H., Tsai, F. S., Godin, J. M. & Lo, Y. H. Human mammalian cell sorting using a highly integrated micro-fabricated fluorescence-activated cell sorter (microFACS). *Lab Chip.* **10**, 1567–1573 (2010).
7. Shapiro, H. M. *Practical Flow Cytometry*, 4th edn. Wiley-Liss (2003).
8. McKenna, B. K., Evans, J. G., Cheung, M. C. & Ehrlich, D. J. A parallel microfluidic flow cytometer for high-content screening. *Nat. Methods* **8**, 401–3 (2011).
9. Conrad, C. *et al.* Micropilot: automation of fluorescence microscopy-based imaging for systems biology. *Nat Methods* **8**, 246–249 (2011).
10. Schneider, A. *et al.* "The good into the pot, the bad into the crop!"--a new technology to free stem cells from feeder cells. *PLoS ONE* **3**(11), e3788 (2008).
11. Wang, W. *et al.* A system for high-speed microinjection of adherent cells. *Rev. Sci. Instrum.* **79**, 104302 (2008).
12. Gellér, Á. Method for sorting fluorescent marked cells. Patent HU 226.930 (2006).
13. Szabó, B. Arrangement for a pipette holding console positioned relative to an objective lens and method for pipette positioning. Patent pending HU P1000339 (2010).
14. Ambriz-Colin, F. *et al.* Detection of biological cells in phase-contrast microscopy images. Fifth Mexican International Conference on Artificial Intelligence Print ISBN: 0-7695-2722-1, 68–77 (2006).
15. Raffael, M., Willert, C. E., Wereley, S. T. & Kompenhans, J. *Particle Image Velocimetry*, Chapter 2.2.1. 2nd edn., Springer (2007).
16. Santiago, J. G., Wereley, S. T., Meinhart, C. D., Beebe, D. J. & Adrian, R. J. A particle image velocimetry system for microfluidics. *Experiments in Fluids* **25**, 316–319 (1998).
17. Sagvolden, G., Giaever, I., Pettersen, E. O. & Feder, J. Cell adhesion force microscopy. *PNAS* **96**, 471–476 (1999).
18. Mollet, M., Godoy-Silva, R., Berdugo, C. & Chalmers, J. J. Computer simulations of the energy dissipation rate in a fluorescence-activated cell sorter: Implications to cells. *Biotechnol Bioeng.* **100**, 260–272 (2008).
19. Berdugo, C. Cell damage mechanisms and stress response in animal cell culture PhD dissertation, Ohio State University, USA, p. 135 (2010).
20. Neumann, B. *et al.* High-throughput RNAi screening by time-lapse imaging of live human cells. *Nat. Methods* **3**, 385–390 (2006).
21. Ziats, N. P., Miller, K. M. & Anderson, J. M. In vitro and in vivo interactions of cells with biomaterials. *Biomaterials* **9**, 5–13 (1998).
22. Kleinfeld, D., Kahler, K. H. & Hockberger, P. E. J. Controlled outgrowth of dissociated neurons on patterned substrates. *Neurosci.* **8**, 4098–4120 (1998).
23. Jung, S. *et al.* Analysis of fractalkine receptor CX(3)CR1 function by targeted deletion and green fluorescent protein reporter gene insertion. *Mol. Cell Biol.* **20**, 4106–4114 (2000).
24. Mosmann, T. J. Rapid colorimetric assay for cellular growth and survival: application to proliferation and cytotoxicity assays. *Immunol. Methods* **65**, 55–63 (1983).

Acknowledgements

Author contributions

Z.K. provided the cell cultures, S.B. developed microfabricated substrates for cell immobilization used in pilot experiments, T.M. performed the numerical simulations, M.J. took part in micropipette pulling, K.J.K. provided the mice for astroglia-microglia cultures, Z.S. prepared fluorescent human leukocytes used in pilot experiments, B.S. performed the experiments and wrote the manuscript.

Additional information

How to cite this article: Környei, Z. *et al.* Cell sorting in a Petri dish controlled by computer vision. *Sci. Rep.* **3**, 1088; DOI:10.1038/srep01088 (2013).